PHILOSOPHICAL MAGAZINE B, 1994, VOL. 70, NO. 6, 1161–1175

Evaluation of multiple-scattering contribution in extended X-ray absorption fine structure for MO_4 and MO_6 clusters

By A. KUZMIN

Institute of Solid State Physics, University of Latvia, LV-1063 Riga, Latvia

and R. GRISENTI

Dipartimento di Fisica, Università di Trento, I-38050 Povo (Trento), Italy

[*Received 4 January 1993*† *and accepted 11 March 1994*]

ABSTRACT

We present a theoretical *ab initio* evaluation of the multiple-scattering contribution in the extended X-ray absorption fine structure for MO_4 and MO_6 clusters with M ≡ Mg, Ca, Mn, Zn, Se, Sr, Mo, Ag, Te, Ba, Nd, Tb, W, Au or Bi. The dependence of the multiple-scattering signal on the absorber type, the photoelectron angular momentum and the local distortion is discussed. It is shown that the multiple-scattering contribution is significant in the photoelectron wave-vector range up to 6–7 $Å^{-1}$ and strongly depends on both the path geometry and the atomic species involved in the scattering process.

§ 1. INTRODUCTION

X-ray absorption spectroscopy (XAS) has become in the last years a powerful tool of local structure study in different materials (Hasnain 1991, Kuroda *et al.* 1993). A considerable number of papers have been devoted to investigation of the local environment in disordered systems (amorphous compounds, glasses and liquids (for example Asakura, Nomura and Kuroda (1985), Benfatto, Natoli, Garcia and Bianconi (1986) and Garcia *et al.* (1989 a))) as well as on surfaces (Baberschke 1989). Usually, in such systems, the signal generated within the first coordination shell gives the main contribution to the observed X-ray absorption fine structure (XAFS) due to high static and/or thermal disorder of outer coordination shells. Its analysis can give us full information about the local order crystallographic parameters as coordination numbers and distributions of distances and angles. Moreover, even when the contribution from outer shells is not negligible, if the first and the second shells are well isolated, as for example in compounds with a perovskite-like structure, then their signals can be easily singled out by Fourier filtering procedure and analysed separately.

From the viewpoint of the multiple-scattering (MS) theory, XAFS can be divided into two ranges: the X-ray absorption near-edge structure (XANES) where the MS series converges slowly and the extended X-ray absorption fine structure (EXAFS) where several first terms of the MS series are enough to simulate it (Ruiz-López *et al.* 1988).

Up to now the exact *ab initio* MS calculations of EXAFS have been performed only for a few number of systems, mainly transition-metal oxides and compounds containing

† Received in final form 20 February 1994.

them (Hasnain 1991, Kuroda *et al.* 1993). In spite of this, several common conclusions concerning the MS contribution have been suggested previously. It was found that the linear or close to linear atomic chains are the origin of the strong MS signal caused by the focusing effect on the intervening atom (Alberding, Crozier, Ingals and Houser 1986, Vedrinskii, Bugaev and Levin 1988, Mustre de Leon *et al.* 1989, Kuzmin, Purans, Benfatto and Natoli 1993). Also it was shown that the MS signal strongly depends on the photoelectron angular momentum for some geometrical configurations (Kuzmin *et al.* 1993) which makes it impossible to use the procedure suggested by Chaboy, Garcia and Marcelli (1992) for the comparison of EXAFS spectra at the $L_{2,3}$ and L_1 edges if the MS contribution is significant.

Two signals generated in the first coordination shell can be distinguished in the experimental EXAFS spectra:

(1) the single-scattering (SS) signal, which produces the main contribution;
(2) the multiple-scattering signal, which modulates the SS signal and appears in the Fourier transform (FT) of EXAFS as a set of peaks at distances longer than the peak due to the SS contribution.

Besides this, even when the contribution from the outer shells is not negligible, the MS signal from the first shell, which is present in any case, coincides in FT with the position of one of the outer (usually second) shells, for example in close-packed structures such as rock salt. Therefore, if the MS signal is sufficiently large in comparison with the SS from the second shell, it complicates analysis of the experimental data, since it cannot be separated by the Fourier filtering procedure. In this case, it has to be taken into account in calculations; otherwise the parameters determined for the second shell will be erroneous.

In this paper we present an evaluation of the MS contribution for tetrahedral MO_4 and octahedral MO_6 clusters (M ≡ Mg, Ca, Mn, Zn, Se, Sr, Mo, Ag, Te, Ba, Nd, Tb, W, Au or Bi). The central atoms (absorbers) were chosen over all the periodic table to show the dependence of the MS signal on the atomic species and the photoelectron angular momentum. The models considered can be applied to a wide class of bulk materials such as amorphous oxides, oxide glasses, aqueous solutions and some crystalline compounds (e.g. perovskites) as well as oxidized surfaces. The results obtained are compared with known experimental data (mainly for aqueous solutions where the second- and outer-shell contributions are negligible) and can be used in the preliminary analysis of the EXAFS spectra for any compounds, especially those in which the structure beyond the first shell is highly disordered, with the purpose of estimating the contribution of the MS processes. Moreover, the present results can be useful to check the validity of the single-shell approximation to the second and outer shells when the amplitude ratio and phase difference analyses are applied (Teo 1986).

§ 2. Method of calculation

The *ab initio* MS calculations were performed using the MSXAS code (Ruiz-López *et al.* 1991, Tyson 1991). It is based on the exact MS theory described previously (Natoli and Benfatto 1986, Ruiz-López *et al.* 1988, Benfatto *et al.* 1989, Brouder *et al.* 1989).

The first step in the *ab initio* calculation of EXAFS is the construction of the total potential for a cluster of given dimension centred on the absorbing atom. In our case, the tetrahedral MO_4 and octahedral MO_6 clusters (M ≡ Mg, Ca, Mn, Zn, Se, Sr, Mo, Ag, Te, Ba, Nd, Tb, W, Au or Bi) were used with the distance R(M–O) = 2·0 Å, which is a typical average coordination radius for MO_x systems (table 1).

Table 1. Atomic coordinates for MO_4 ($a = R(M–O)/3^{1/2}$) and MO_6 ($a = R(M–O)$) regular clusters.

Cluster	Atom	x	y	z
MO_4	M(0)	0	0	0
	O(1)	a	a	a
	O(2)	$-a$	$-a$	a
	O(3)	$-a$	a	$-a$
	O(4)	a	$-a$	$-a$
MO_6	M(0)	0	0	0
	O(1)	a	0	0
	O(2)	$-a$	0	0
	O(3)	0	a	0
	O(4)	0	$-a$	0
	O(5)	0	0	a
	O(6)	0	0	$-a$

The details of cluster potential calculation have been described previously by Ruiz-López *et al.* (1988) and Tyson (1991). Briefly, the total cluster potential was constructed from a set of spherically averaged *muffin-tin* (MT) potentials, which were built following to the standard Mattheiss (1964) prescription; the atomic charge densities obtained from self-consistent solutions of the single-electron relativistic Dirac equations were placed on each atomic site in the cluster, and the superposed charge density was spherically averaged about the atom whose potential was required. Then the Poisson equation for the Coulomb part of the potential was solved, and the complex Hedin–Lundqvist (1971) exchange–correlation potential, based on the density functional formalism within the single-plasmon pole approximation, was added. The latter allows one to take into account the EXAFS amplitude damping associated with the inelastic losses of the photoelectron in extrinsic channels on plasmon excitations.

The values of the MT radii were chosen according to the Norman (1974) criterion with overlap factor of about 10%. The final state of the absorbing atom was taken to be fully relaxed with a hole localized in the appropriate core site (in the 1s level for the K edge, in the 2s level for the L_1 edge and in the $2p_{3/2}$ level for the L_3 edge).

Further, the Schrödinger radial equations were solved locally by a numerical method for each atom of the cluster, and the normalized radial solutions R_l were obtained. The atomic **T**-matrix elements t_l used in the scattering amplitude calculations were found in the usual way by matching R_l functions with solution for free space at the MT-spheres boundary (Ruiz-López *et al.* 1988).

In the MS expansion, the EXAFS signal χ^l above the absorption edge of orbital type l ($l = 0$ for the K, L_1 edges and $l = 1$ for the $L_{2,3}$ edges) can be described by the scattering series (Natoli and Benfatto 1986, Ruiz-López *et al.* 1988)

$$\chi^l = \sum_{n=2}^{\infty} \chi_n^l, \tag{1}$$

with

$$\chi_n^l = \sum_i A_i^l(k, R_i) \sin(2kR_i + \Phi_i^l(k, R_i) + 2\delta_c^l), \tag{2}$$

where χ_n^l represents contributions from all processes, where the excited photoelectron

Table 2. Scattering paths (χ_2, SS; χ_3, DS; χ_4, TS) used in MS calculations for MO_4 and MO_6 regular clusters. The numbers in the paths correspond to the atoms in table 1.

Type	Process	Path	Degeneracy	Effective distance
		MO_4		
χ_2	SS	0–1–0	4	R
χ_3	DS	0–1–2–0	12	$\approx 1{\cdot}8R$
χ_4	TS1	0–1–0–1–0	4	$2R$
	TS2	0–1–0–2–0	12	$2R$
	TS3	0–1–2–1–0	12	$2{\cdot}6R$
	TS4	0–1–2–3–0	24	$2{\cdot}6R$
		MO_6		
χ_2	SS	0–1–0	6	R
χ_3	DS1	0–1–2–0	6	$2R$
	DS2	0–1–3–0	24	$\approx 1{\cdot}7R$
χ_4	TS1	0–1–0–1–0	6	$2R$
	TS2	0–1–0–2–0	6	$2R$
	TS3	0–1–0–3–0	24	$2R$
	TS4	0–1–3–1–0	24	$2{\cdot}4R$
	TS5	0–1–3–5–0	48	$2{\cdot}4R$

experiences $n-1$ scatterings by the surrounding atoms before returning to the absorber; Σ_i means the sum over all paths of order n starting from and terminating at the absorber; R_i indicates the path length; $A_i^l(k, R_i)$ and $\Phi_i^l(k, R_i)$ are the effective amplitude and phase functions, which depend on the wave-vector k of the photoelectron, the angular momentum l, the length and geometry of the path and the nature of the scattering centres; δ_c^l is the phase shift due to the absorbing (central) atom.

Usually only a few terms of the series (1) produce significant contributions to the total signal, especially at high energies because of such factors as the path length ($1/R^2$ factor in the amplitude), the finite lifetime of the excitation (both the photoelectron mean free path and the core hole lifetime affect the amplitude value by a factor $\exp(-2R/\lambda_{\text{effective}})$) and destructive interference between different oscillating signals. In this work, the first three terms, corresponding to the processes of SS (χ_2^l), double scattering (DS) (χ_3^l) and triple scattering (TS) (χ_4^l) (table 2), were calculated in the exact curved-wave approach (Natoli and Benfatto 1986, Ruiz-López *et al.* 1988) by the MSXAS code. It is necessary to point out that the MS contribution can extend as far as about 6–7 Å^{-1}, that is up to the middle of the usual EXAFS spectrum range.

The FT procedure of the EXAFS $\chi(k)k^2$ signal with a Gaussian window, $\exp(-Ak^2)$ with $A = 0{\cdot}05$, centred at the midpoint of the data range $k = 0$–12 Å^{-1}, was used to show the behaviour of the EXAFS signal in R space. The FT is the analogue of the many-body distribution function except that the peak positions are shifted from their true crystallographic values owing to the presence of the $\Phi_i^l(k, R_i) + 2\delta_c^l$ phase shift in eqn. (2).

In present calculations the Debye–Waller (DW) factor was *not* included, and the amplitude of the calculated signals is smaller in the case of real systems owing to the thermal damping term of the $\exp(-2\sigma^2_{\text{effective}}k^2)$ type. The influence of the DW factor on the amplitude of XAFS function in particular case of MO_x clusters will be discussed in § 3.

In reality, except for the thermal damping, the broadening effects owing to limited experimental resolution and finite lifetime of the excitation can also influence on the XAFS amplitude mainly at low energies. In particular, very low experimental resolving power ($\Delta E \approx 5$–6 eV), for example for K edges of heavy elements and often for laboratory EXAFS spectrometers, can lead to the 'disappearance' of the first-shell MS signals which contribute at the beginning of the XAFS spectrum.

Note that, even when the amplitude of a peak in FT is negligibly small, it does not mean that the contribution of such signal is negligible in XAFS too. The reason is that the distribution of amplitudes in FT is strongly affected by such factors as limited interval of XAFS, the transform 'window' and the weight factor k^n.

§ 3. Results and discussion

This section is devoted to the results of MS calculations for MO_4 and MO_6 clusters with M ≡ Mg, Ca, Mn, Zn, Se, Sr, Mo, Ag, Te, Ba, Nd, Tb, W, Au or Bi and their comparative analysis. The central metal atoms were chosen over all the periodic table. Owing to the smooth dependence of the central atom scattering phase on atomic number, the presented results can be easily transferred to intermediate elements. The main idea is to show how the contribution from the MS processes responds to firstly the change in the central atom type, secondly the photoelectron angular momentum and thirdly the cluster distortion. It will be shown that the existing opinion that the MS contribution is very small in tetrahedral coordination and becomes significant in octahedral coordination owing to the appearance of linear chains is not fully true and depends strongly on the above-mentioned conditions. Moreover, we shall show that the total contribution from the MS signals is less sensitive to the local distortions than is the contribution from the SS signals. This can be useful for studying well known *off centre* problem (Mustre de Leon *et al.* 1989).

The MO_4 cluster is the basic unit for a great number of real compounds, for example spinels, glasses, amorphous materials and solutions. The O–M–O angle is equal to about 109·5° which is sufficiently far from the value of 180° in the linear chain. Therefore it could seem that MS signal in EXAFS has to be small (Lee and Pendry 1975). Later it was found (Benfatto *et al.* 1986) that the third-order MS signal is present in the case of MnO_4 tetrahedral complexes in aqueous solution, and it was related to the DS process of the metal → ligand (1) → ligand (2) → metal type. The conclusion was drawn (Garcia, Bianconi, Benfatto and Natoli 1986) that the MS higher-order terms in MO_4 tetrahedral clusters go to zero more quickly than in octahedral clusters, and the destructive interference effect between pairs of consecutive terms, that is χ_n and χ_{n+1}, does not take place as in octahedral coordination. Here we shall show that the last conclusion is not true in the general case, and a strong correlation of the MS contribution in MO_4 with the absorber type and the angular momentum of the photoelectron occurs.

The MO_6 clusters are present as basic units in a wide range of materials, especially those containing transition-metal oxides. In 'pure' form they can be found in aqueous solutions (Asakura *et al.* 1985, Garcia *et al.* 1989a, Karim, Harget and Saw 1989, Sanchez del Rio *et al.* 1990, Muñoz-Paez and Sánchez 1992, Read and Sandström 1992) where the MS contribution is easily visible when the signal-to-noise ratio is sufficiently large (Asakura *et al.* 1985, Garcia *et al.* 1989a, Muñoz-Paez and Sánchez 1992). Unlike the MO_4 case, the presence of linear chains leads to a focusing effect on the intervening atom (absorber) (Garcia *et al.* 1989a). Several papers have been published previously concerning the interpretation of XAFS in the MO_6 clusters mainly with regular structure (for example Garcia *et al.* (1986, 1989a, b) and Sanchez del Rio *et al.* (1990)). The

agreement achieved between theoretical calculations in the MS formalism and experimental data was reasonable. It was found that XAFS spectra of octahedral complexes can be described in the SS formalism only in first approximation. The precise description needs the inclusion of the MS processes. In particular, the MS contribution was found to be quite significant in the k space (k is the wave-vector of the photoelectron) near the absorption edge and in the R space (in FT of XAFS) at distances about twice the average distance in the first shell. Note that the MS contribution to the FT can be more than 15% of the first-shell signal and varies from system to system (see, for example, fig. 1 (*b*) of the paper by Garcia *et al.* (1989a)). It was concluded that the MS contribution depends on the particular case because of the strong interference effects between different MS signals.

In this paper, the results obtained are presented in a compressed form with the aim of saving space. More detailed information can be obtained directly from the authors.

The FTs of the total EXAFS signals and of separate MS signals $\chi_n(k)k^2$ ($n = 2, 3, 4$) for regular MO_4 and MO_6 clusters are shown in fig. 1. The MS contributions in k space extend to about 6–7 $Å^{-1}$ and give rise to peaks in FT located between about 2 and about 4–5 Å. The behaviours of different MS signals differ in some cases only in phase (SS, DS, TS3 and TS4 in tetrahedral clusters and SS, DS1, DS2, TS4 and TS5 in octahedral clusters) but in other cases (TS1 and TS2 in tetrahedral clusters and TS1, TS2 and TS3 in octahedral clusters), when the central atom not only is the origin and terminal point of the scattering path but also perturbs the photoelectron wave at the intermediate moments of time, there is significant difference both in the phase and in the amplitude. In particular, the TS1 signal, corresponding to the $M \rightarrow O(1) \rightarrow M \rightarrow O(1) \rightarrow M$ path, has the smallest contribution in the case of the K-edge EXAFS for transition elements of the third period (fig. 2 (*a*)) and in the case of the $L_{1,3}$ edges EXAFS for elements from tungsten to gold (figs. 2 (*b*) and (*c*)). The behaviour of the TS2 signal, corresponding to the $M \rightarrow O(1) \rightarrow M \rightarrow O(2) \rightarrow M$ path with an O(1)–M–O(2) angles of 109·5° and 180° for tetrahedral and octahedral clusters respectively, is more complicated. In the case of the K-edge EXAFS, it decreases from magnesium to manganese, increases to selenium and decreases again to tellurium (fig. 2 (*a*)). Thus the TS2 signal is as small for the transition elements of the third period as TS1 and decreases along the fourth period. Note that such behaviour is the same in the case of both MO_4 and MO_6 clusters. In the case of the $L_{1,3}$-edge EXAFS, the TS2 signal decreases when the central element becomes heavier except for the L_3 edge in the MO_4 cluster where it increases after gold (figs. 2 (*b*) and (*c*)). The last TS signal $M \rightarrow O(1) \rightarrow M \rightarrow O(2) \rightarrow M$ (TS3) with an O(1)–M–O(2) angle of 90°, which exists only in the MO_6 clusters, differs significantly for the K, L_1 and L_3 edges. For the K edge the TS3 signal is the smallest for elements from calcium to manganese and increases to tellurium (fig. 2 (*a*)). For $L_{1,3}$ edges the TS3 signal is proportional to the atomic number of the central atom (figs. 2 (*b*) and (*c*)); when the atomic number increases, the TS3 signal increases for the L_1 edge and decreases for the L_3 edge.

The comparison of FTs of the total EXAFS signals (fig. 1) allows one to draw several conclusions. The total MS contribution is represented by peaks located to the FT between 2 and 4 Å. The smallest amplitude of the MS signal is in MO_4 clusters for the L_3 edge, and it is the largest in MO_6 clusters for $L_{1,3}$ edges. In other cases the amplitude of the peaks corresponding to the MS contribution has an intermediate value and depends strongly on the central atom type. For example, it is very small for the Se K edge in the SeO_4 cluster whereas it becomes comparable with the MS contribution in octahedral clusters for the Ca and Mn K edges in CaO_4 and MnO_4 respectively.

Fig. 1

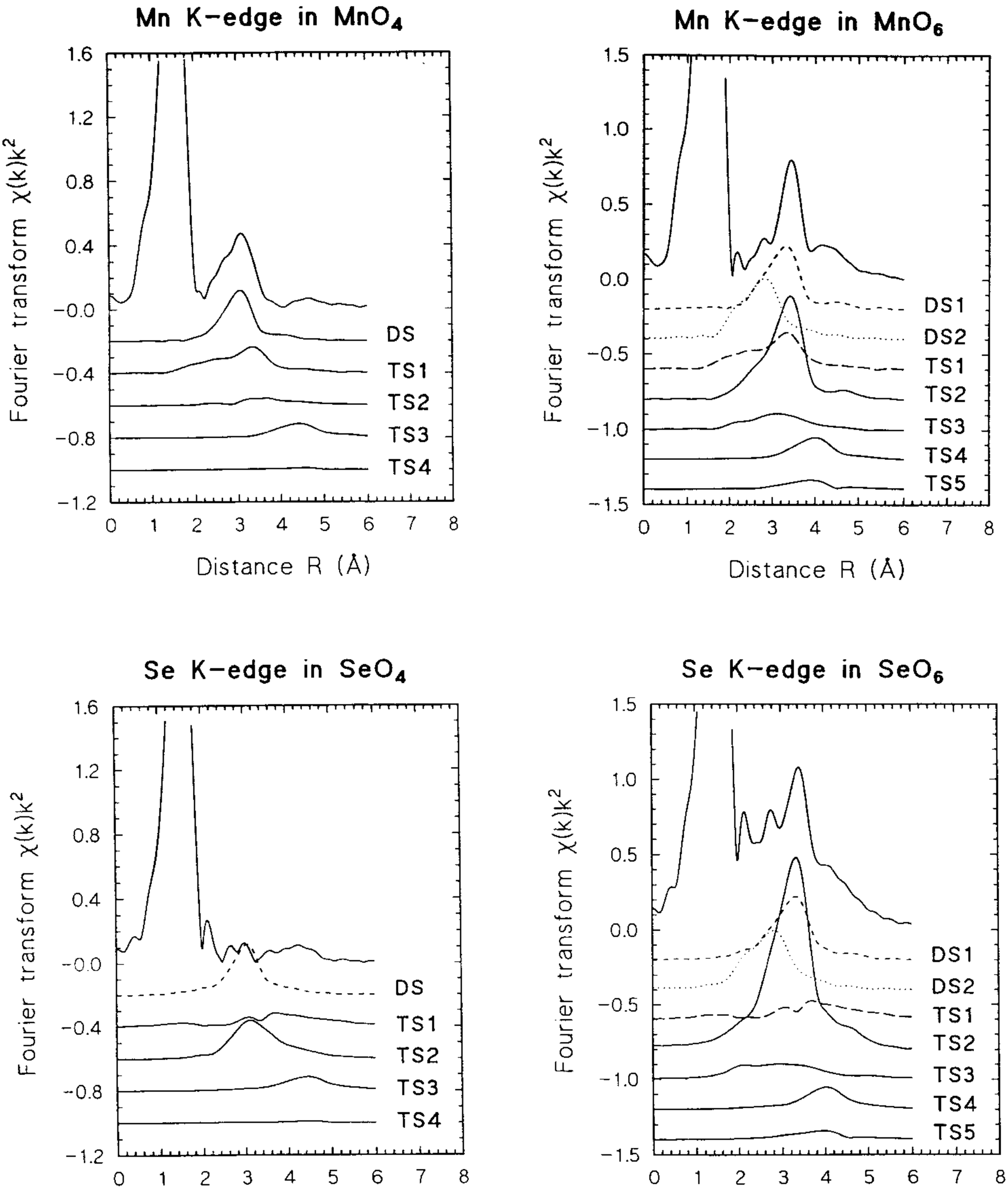
Mn K–edge in MnO_4
Mn K–edge in MnO_6
Se K–edge in SeO_4
Se K–edge in SeO_6
Fourier transform $\chi(k)k^2$
Distance R (Å)
DS
TS1
TS2
TS3
TS4
DS1
DS2
TS5

(*a*)

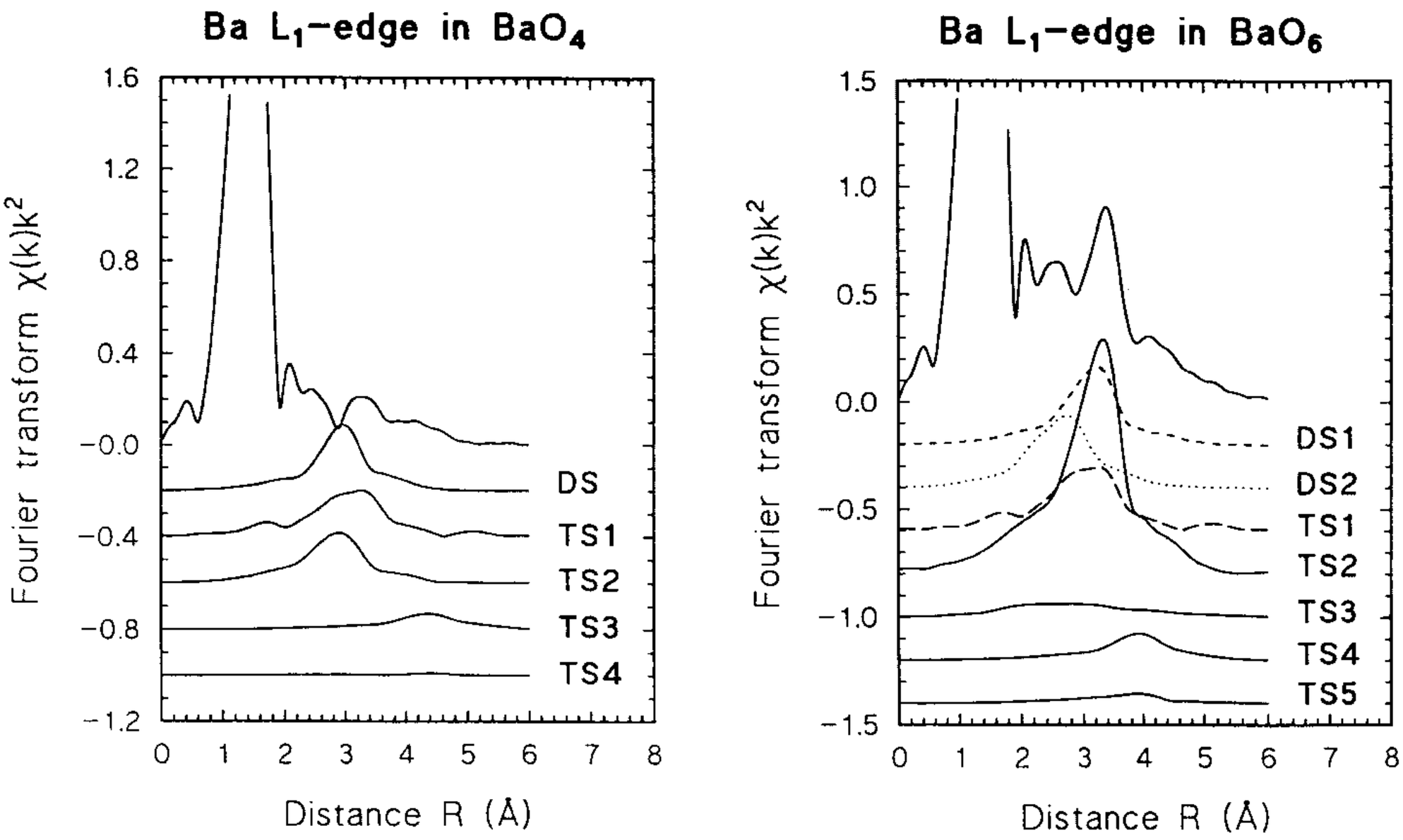
Ba L1–edge in BaO4
Ba L1–edge in BaO6
Fourier transform χ(k)k2
Distance R (Å)
DS
TS1
TS2
TS3
TS4
DS1
DS2
TS5

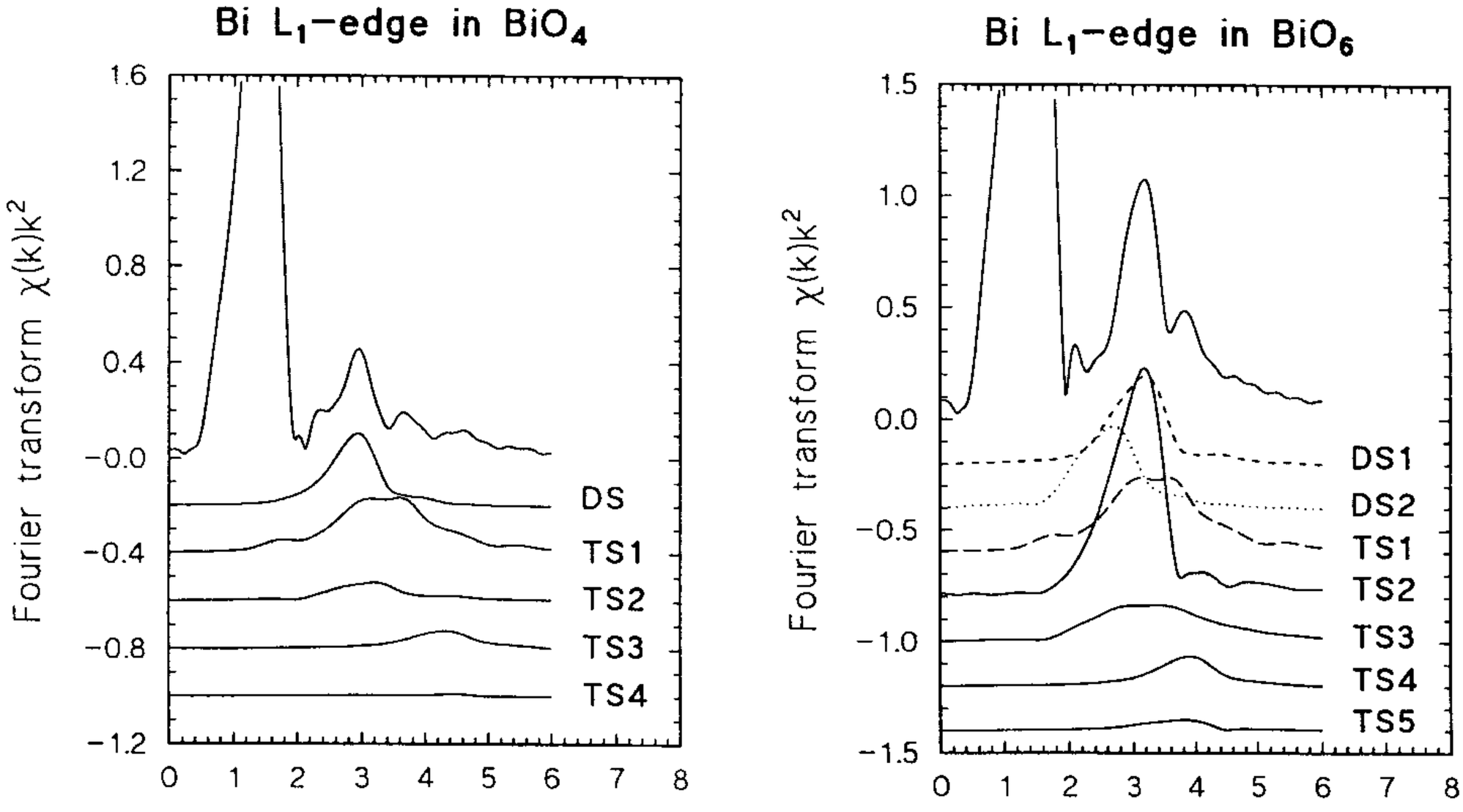
Bi L1–edge in BiO4
Bi L1–edge in BiO6
Fourier transform χ(k)k2
Distance R (Å)
DS
TS1
TS2
TS3
TS4
DS1
DS2
TS5

(b)

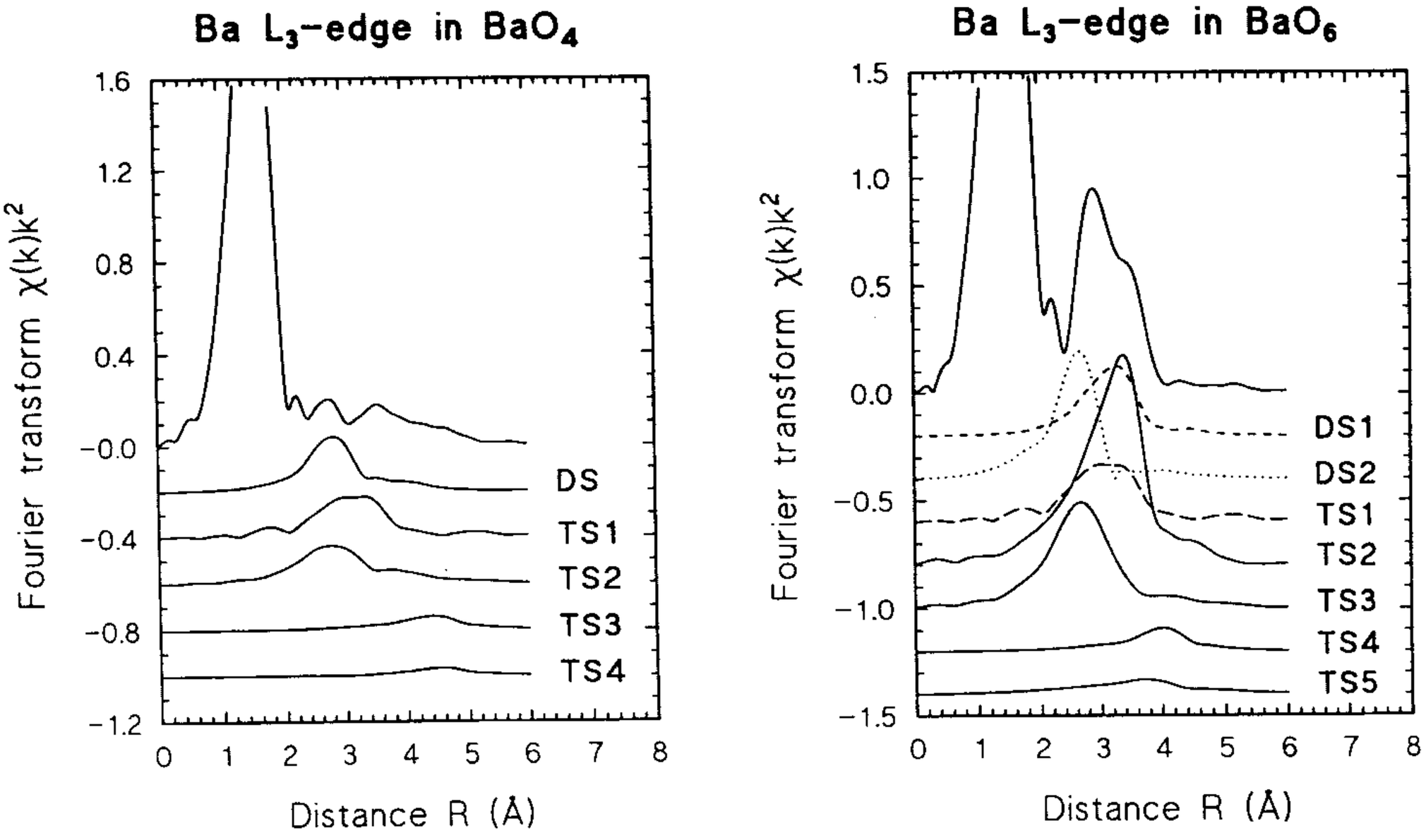

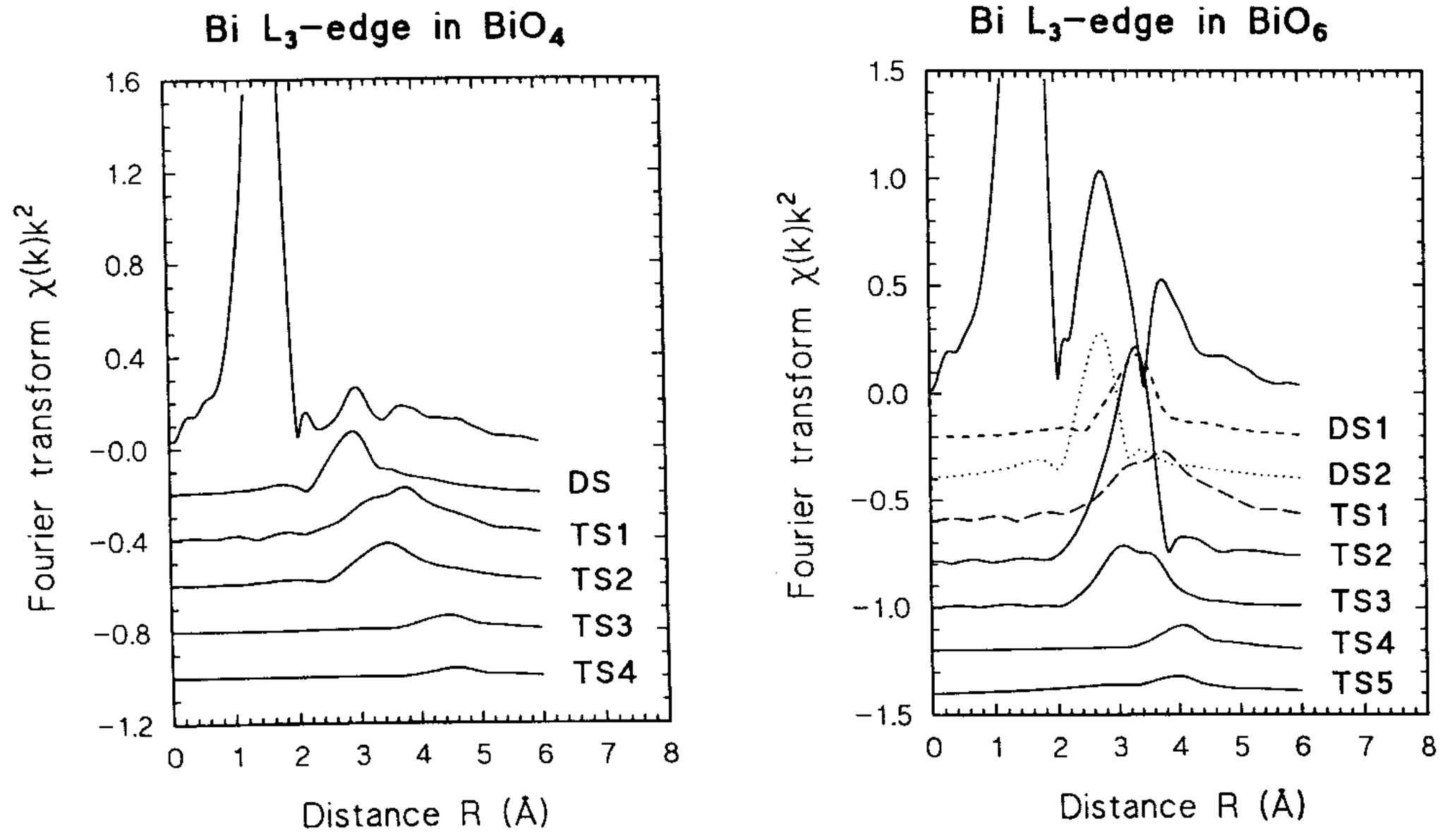

(*c*)

Fourier transforms of the total EXAFS $\chi(k)k^2$ signals and separate MS contributions in regular clusters: (*a*) Mn and Se K edges in MO_4 and MO_6; (*b*) Ba and Bi L_1 edges in MO_4 and MO_6; (*c*) Ba and Bi L_3 edges in MO_4 and MO_6. The definition of MS signals is given in table 2.

Fig. 2

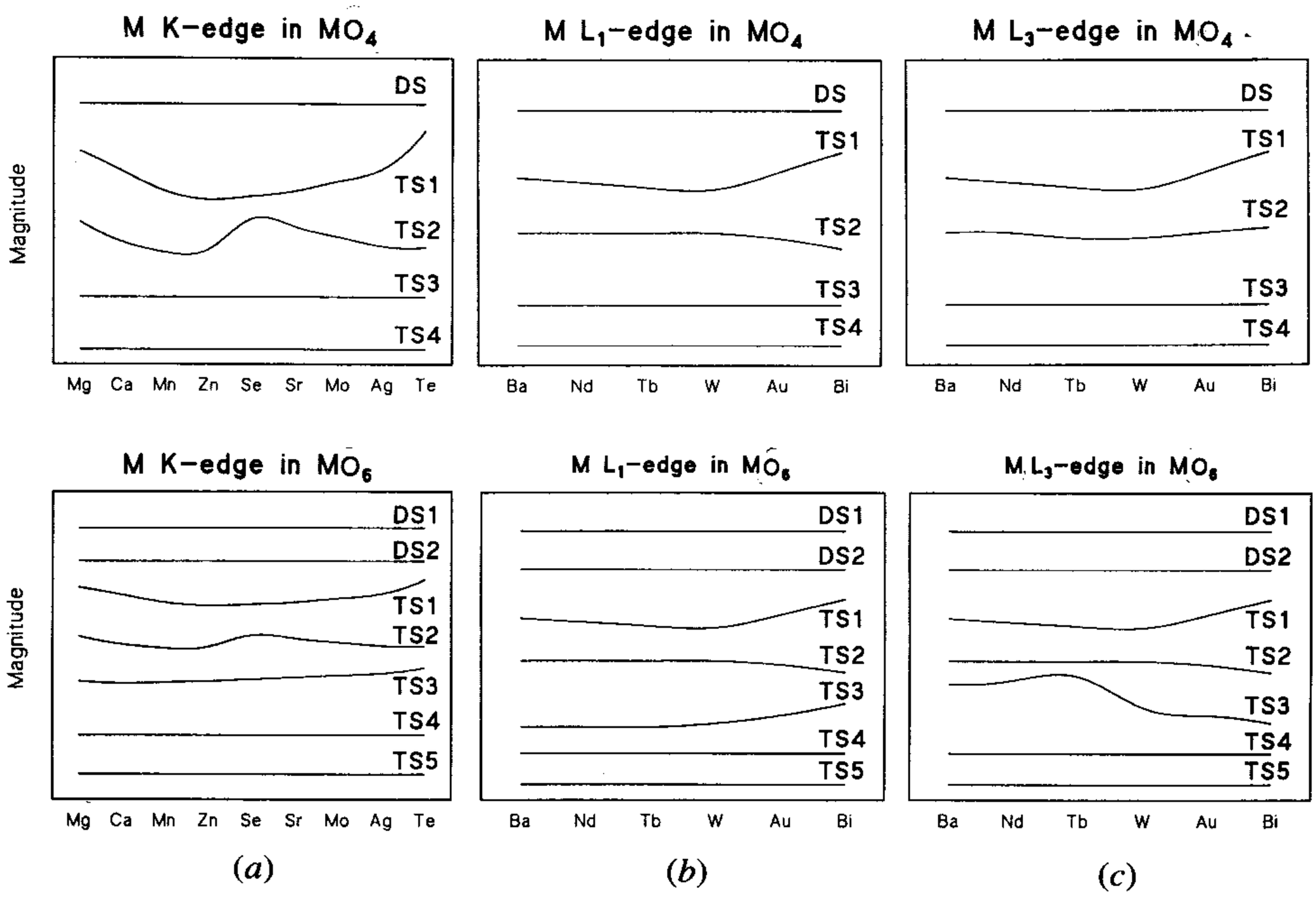

The qualitative behaviour of the MS χ_n signal maxima in MO_4 and MO_6 clusters for the K and $L_{1,3}$ edges. One can see that variation in the MS signal amplitude is present only for the MS paths involving the absorber atom at the intermediate moments of time (TS1 and TS2 in MO_4 clusters and TS1, TS2 and TS3 in MO_6 clusters).

To make the picture clearer, let us consider how separate MS signals contribute to the FT (fig. 1). In the case of MO_4 clusters, the DS, TS1 and TS2 signals produce the main contributions. Nevertheless the amplitudes of the TS1 and TS2 signals depend on both the central atom type and the edge, whereas the FTs of the DS signals are the same in all cases. The reason for this behaviour of the TS1 and TS2 signals is destructive interference effects between different MS signals. This conclusion is opposite to that of Garcia *et al.* (1986). They considered only the example of the 3d transition-metal K edge in MO_4 clusters. In that case the destructive interference effect is small, but this is not true in the general case.

In MO_6 clusters the main contributions are produced by the DS1, DS2, TS1, TS2 and TS3 signals where the TS1 signal, corresponding to the focusing effect in an O(1)–M–O(2) linear chain, has the largest amplitude. Note that the TS1 signal has the opposite phase to the DS contribution which is the reason for the destructive interference observed previously (Garcia *et al.* 1986, 1989a). Three signals DS2, TS1 and TS3 depend strongly on the central atom and the edge type, whereas the TS1 signal, corresponding to the $M \rightarrow O(1) \rightarrow M \rightarrow O(1) \rightarrow M$ scattering process, depends mainly on the central atom type and becomes larger for the elements of the sixth period (from Ba to Bi). Two other signals DS2 and TS3 show a strong dependence on the photoelectron angular momentum; their amplitudes are smaller for K and L_1 edges, that is for photoelectrons with p symmetry. This effect was observed previously for ReO_3 and $NaWO_3$ crystals (Kuzmin *et al.* 1993, Kuzmin and Purans 1993). The reason is that both DS2 and TS3 signals correspond to the O(1)–M–O(2) chain with an O(1)–M–O(2) angle of 90°. In the plane-wave approximation this effect follows straightforwardly

from the cancellation of the DS2 and TS3 terms owing to the zero value of the Legendre polynomial ($P_l(\cos\theta) = 0$ when $l = 1$ and $\theta = 90°$). In the case of the exact curved-wave approach the DS2 and TS3 signals do not disappear completely but differ sufficiently for the K, L_1 and L_3 edges (Kuzmin *et al.* 1993). The variation in the amplitude is more significant for the TS3 signal where the photoelectron experiences scattering on the 90° angle twice. This result is very important for the comparison analysis of EXAFS spectra for L_1 and L_3 edges. In particular, it means that, when the MS contribution is significant, it is not possible to use the procedure suggested by Chaboy *et al.* (1992) to reconstruct one spectrum from another.

Further, we shall discuss the influence of the different kinds of cluster distortion on the XAFS in MO_4 and MO_6 clusters. Calculations were done for several MO_4 and MO_6 clusters with different central atoms and, as an example, we present here the results only for the WO_x cluster where both symmetries of the photoelectron (p ($l = 1$) and d ($l = 2$)) exist.

The results of the calculations for distorted WO_4 clusters for both the L_1 and the L_3 edges are presented in figs. 3 (*a*) and (*b*). The distortion of the regular cluster was produced by the shift of W along the W–O bond to O and in the opposite direction. The values of the shift were 5 and 10% from the W–O bond length. Peak (1) corresponds to the SS processes in the first coordination shell, and label (2) indicates the region of the MS contribution. One can see that the shift of the W atom in the direction of O leads to greater distortion of the first-shell contribution. The enlarged MS region is shown in fig. 3 (*c*). A, B and C indicate the approximate positions of the MS contributions corresponding to the following processes: A, $W \rightarrow O(1) \rightarrow O(2) \rightarrow W$; B, $W \rightarrow O(1) \rightarrow W \rightarrow O(1) \rightarrow W$; C, $W \rightarrow O(1) \rightarrow W \rightarrow O(2) \rightarrow W$. The first is DS, and the last two are TS processes. One can see that the shift of W from the centre of the WO_4 tetrahedron leads to the significant rearrangement of the FT peaks corresponding to the MS signals.

The results for the distorted MO_6 clusters are shown for the example of WO_6 in fig. 4. Three distortions, which correspond to the shift of W in the [100], [110] and [111] directions, were considered. The simple comparison of the SS and MS contributions shows that the MS signals are less sensitive to the distortion. While the first peak at about 1·4 Å corresponding to the SS signal changes its shape greatly from the symmetric shape for the regular cluster to the double-hump structure for the distorted case, the shape of the MS signal remains more or less unchanged especially for the L_1 edge where only the amplitude decreases with distortion. For the L_3 edge, more prominent changes are observed at the left-hand side of the peak at about 2·6 Å. This result proves the conclusion drawn above concerning different contributions of the DS2 signal in the case of the L_1 and L_3-edge EXAFS. The high amplitude of the DS2 signal is due to its large degeneracy. When distortion occurs, the set of DS2-like paths splits into several groups whose sum becomes very small and this influences the shape of the peak in FT at about 2·6 Å.

As was emphasized in § 2, the amplitude of experimental XAFS signals is decreased by thermal damping term, $\exp(-2\sigma^2_{\text{effective}}k^2)$. There are two consequences of this type of damping: firstly it affects more strongly the amplitude of oscillations at high energies where the contribution from the SS signal dominates compared with the MS signal, and secondly, because the MS contribution in MO_x clusters is negligible beyond about 7 $Å^{-1}$, the increase in the DW factor $\sigma^2_{\text{effective}}$ leads in this region mainly to a decrease in the SS signal amplitude. Since the FT is an integrated characteristic over all energy range, therefore, in the particular case of MO_x clusters, when the DW factor appears

Fig. 3

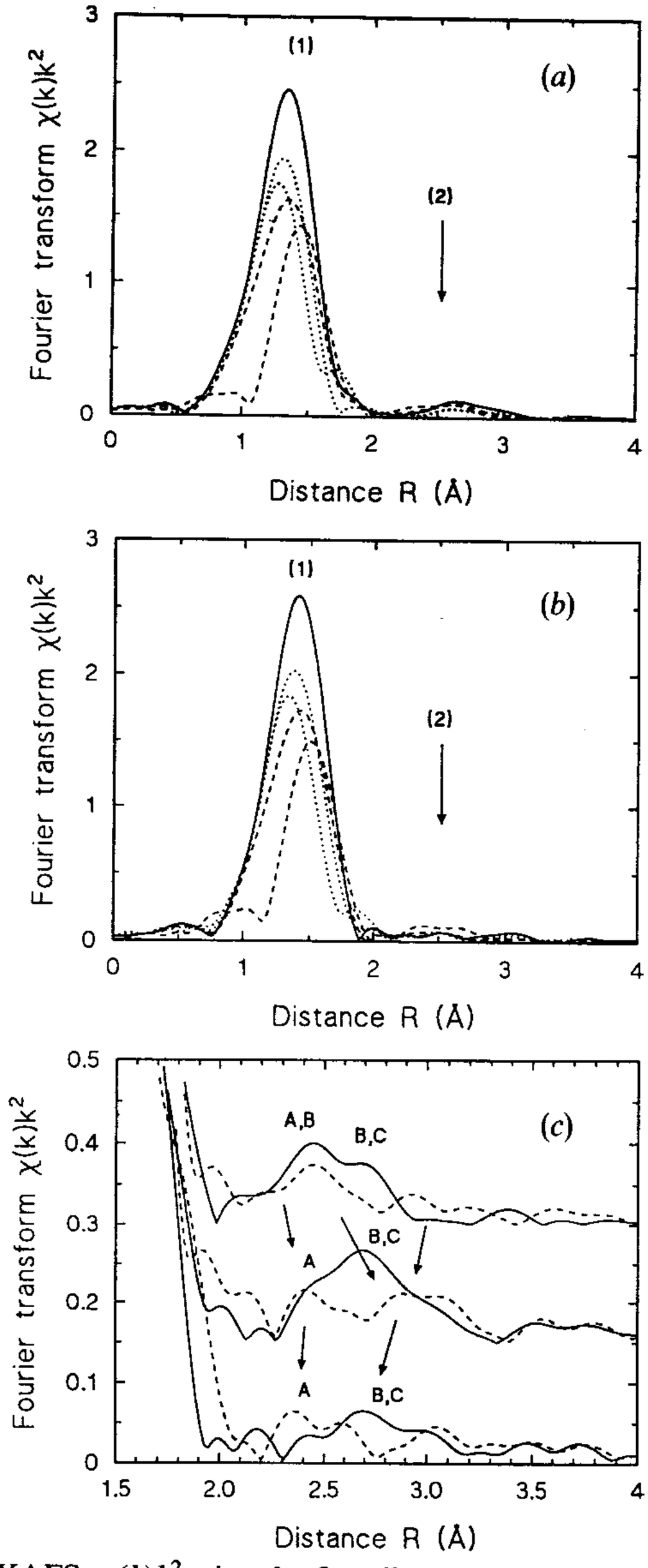

FTs of the total EXAFS $\chi(k)k^2$ signals for distorted WO_4 clusters. (*a*) L_1 edge of W: (——), regular cluster; (– – –), (· · · · ·), distorted cluster. The distortion was produced by the shift of the W along the W–O bond to O (– – –) and in the opposite direction (· · · · ·). The higher-amplitude curves correspond to the less distorted cluster. (*b*) The same as (*a*) only for the L_3 edge of W. (*c*) The enlarged region of MS contribution: upper curves, the W ion is shifted along the W–O bond in the direction of O; middle curves, the regular cluster; lower curves, the W ion is shifted along the W–O bond in the direction opposite to O; (——), L_1 edge of W; (– – –), L_3 edge of W.

Fig. 4

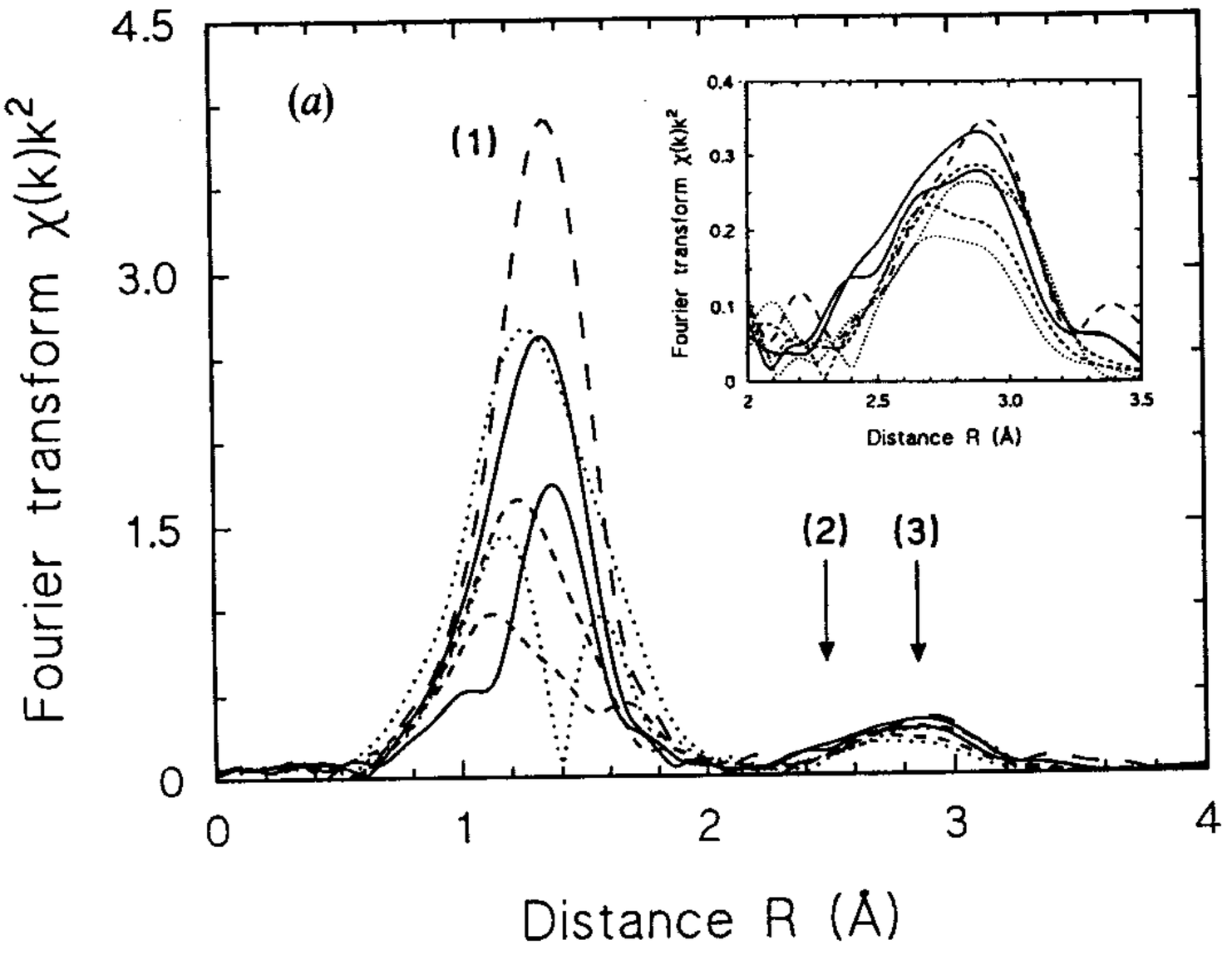

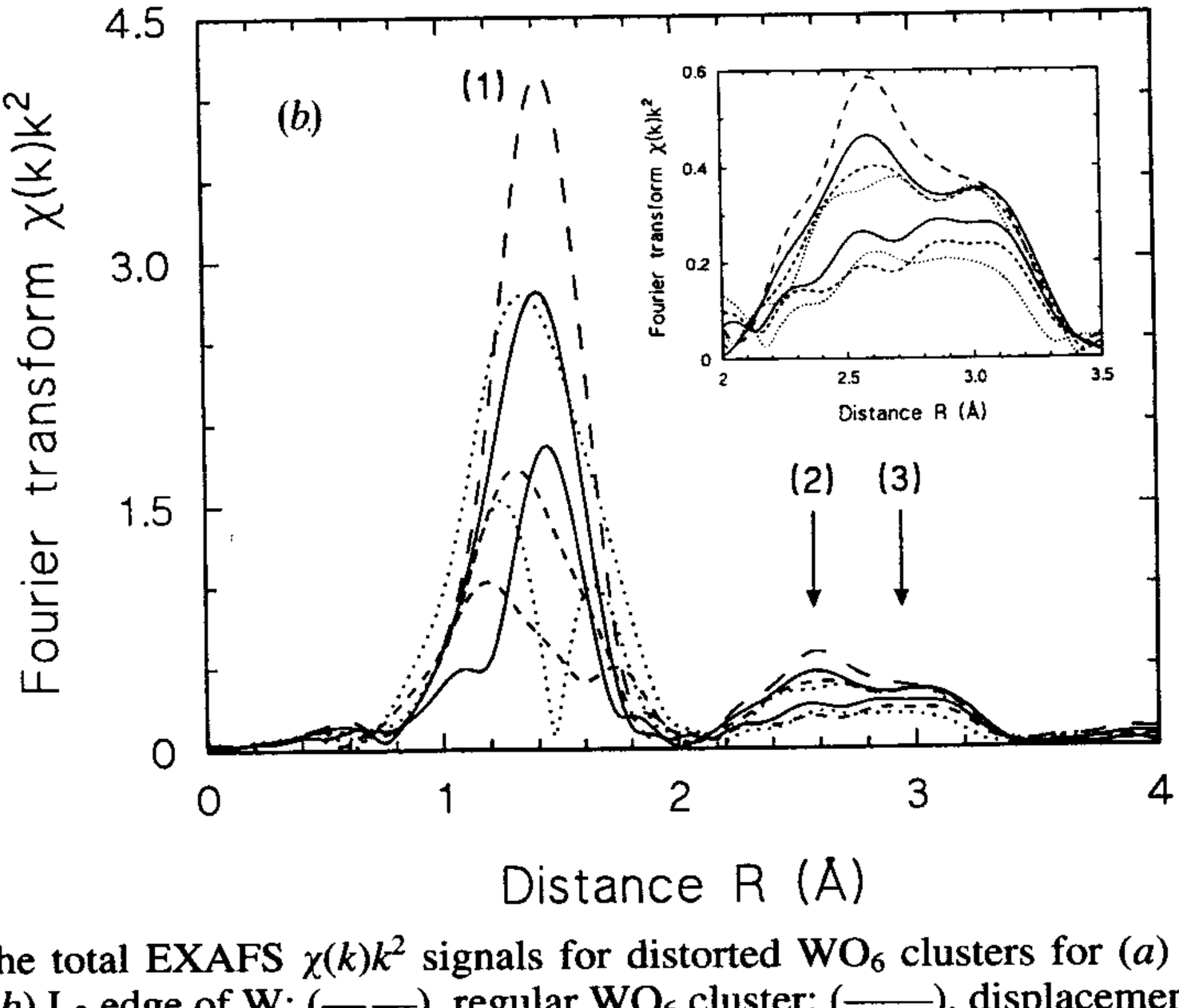

FTs of the total EXAFS $\chi(k)k^2$ signals for distorted WO_6 clusters for (*a*) L_1 edge of W and (*b*) L_3 edge of W: (——), regular WO_6 cluster; (——), displacement Δ of the tungsten in the [100] direction (upper curve, $\Delta = 0{\cdot}05R_{M-O}$; lower curve, $\Delta = 0{\cdot}10R_{M-O}$); (– – –), displacement in the [110] direction (upper curve, $\Delta = 0{\cdot}05R_{M-O}$; lower curve, $\Delta = 0{\cdot}10R_{M-O}$); (· · · ·), displacement in the [111] direction (lower curve, $\Delta = 0{\cdot}05R_{M-O}$; upper curve, $\Delta = 0{\cdot}10R_{M-O}$). Three main contributions are indicated: (1) SS; (2) mainly DS; (3) DS plus TS. The region of the MS contributions is enlarged.

for both SS and MS contributions (in spite of the fact that its value is usually larger for the MS signals), the *relative* change in the SS and MS peaks amplitude in FT compared with the case of $\sigma^2_{\text{effective}} = 0$ is expected to be nearly the same.

§ 4. Summary and conclusions

In this paper we present the evaluation of the MS contributions in MO_4 and MO_6 (M ≡ Mg, Ca, Mn, Zn, Se, Mo, Ag, Te, Ba, Nd, Tb, W, Au or Bi) clusters. The K, L_1 and L_3 edges are considered depending on the absorber. It is shown that the amplitude of the MS signals correlates strongly with the absorber type and the photoelectron angular momentum. In particular, as was expected, the change in the absorber modifies the phase of the XAFS signals (both SS and MS) owing to the change in the central atom phase shift, and also the variation in the MS signal amplitude is present only for MS paths involving the absorber atom at the intermediate moments of time. The destructive interference between the MS signals plays an important role for both MO_4 and MO_6 clusters. In spite of the fact that the MS contribution in most cases is greater in octahedral coordination, it cannot be neglected for tetrahedral clusters too.

The effect of distortion on the MS signal generated within MO_4 and MO_6 clusters was considered for the example of W $L_{1,3}$-edge EXAFS. The distortion of the WO_4 cluster leads to a complex change in the total MS signal without a significant influence on its amplitude. For the WO_6 cluster, the distortion influences mainly the SS contribution and the DS signal of triangle type (W → O(1) → W → O(3) → W; O(1)–W–O(2) angle, 90°). The last contribution is also the most sensitive to the change in the photoelectron angular momentum. Similar behaviours were observed in the case of other central atoms.

Thus the analysis of the experimental EXAFS signals from atoms beyond the first shell has to take into account the MS contribution at least if the energy range below 6–7 $Å^{-1}$ is analysed. Note that, when the MS contribution is not taken into account, it can lead to the erroneous interpretation of experimental data; for example, for aqueous solutions the peaks corresponding to the MS signal can be erroneously taken for the outer hydration shells (Muñoz-Paez and Sánchez 1992).

Acknowledgments

The authors are grateful to Professor C. R. Natoli and co-workers for the possibility of using the MSXAS code. They wish to thank Professor P. Fornasini for critical reading of the manuscript. One of us (A.K.) would like to thank the University of Trento (Professor G. Dalba) and Centro Consiglio Nazionale delle Ricerche di Fisica degli Stati Aggregati ed Impianto Ionico (Dr F. Rocca) for hospitality and financial support.

References

Alberding, N., Crozier, E. D., Ingals, R., and Houser, B., 1986, *J. Phys., Paris*, **47,** C8–681.
Asakura, K., Nomura, M., and Kuroda, H., 1985, *Bull. chem. Soc. Japan*, **58,** 1543.
Baberschke, K., 1989, *Physica* B, **158,** 19.
Benfatto, M., Natoli, C. R., Garcia, J., and Bianconi, A., 1986, *J. Phys., Paris*, **47,** C8–25.
Benfatto, M., Natoli, C. R., Brouder, C., Pettifer, R. F., and Ruiz-López, M. F., 1989, *Phys. Rev.* B, **39,** 1936.
Brouder, C., Ruiz-López, M. F., Pettifer, R. F., Benfatto, M., and Natoli, C. R., 1989, *Phys. Rev.* B, **39,** 1488.
Chaboy, J., Garcia, J., and Marcelli, A., 1992, *Solid St. Commun.*, **82,** 939.
Garcia, J., Benfatto, M., Natoli, C. R., Bianconi, A., Fontaine, A., and Tolentino, H., 1989b, *Chem. Phys.*, **132,** 295.
Garcia, J., Bianconi, A., Benfatto, M., and Natoli, C. R., 1986, *J. Phys., Paris*, **47,** C8–49.

GARCIA, J., SANCHEZ DEL RIO, M., BURATTINI, E., BENFATTO, M., and NATOLI, C. R., 1989a, *Physica* B, **158,** 409.
HASNAIN, S. S. (editor), 1991, *Proceedings of the Sixth International Conference on X-ray Absorption Fine Structure* (Chichester, West Sussex: Ellis Horwood).
HEDIN, L., and LUNDQVIST, B. I., 1971, *J. Phys.* C, **4,** 2064.
KARIM, D. P., HARGET, P. J., and SAW, C. K., 1989, *Physica* B, **158,** 47.
KURODA, H., OHTA, T., MURATA, T., UDAGAWA, Y., and NOMURA, M. (editors), 1993, *Proceedings of the Seventh International Conference on X-ray Absorption Fine Structure* (*Jap. J. appl. Phys., Suppl. 2,* **32**).
KUZMIN, A., and PURANS, J., 1993, *J. Phys.: condens. Matter*, **5,** 267.
KUZMIN, A., PURANS, J., BENFATTO, M., and NATOLI, C. R., 1993, *Phys. Rev.* B, **47,** 2480.
LEE, P. A., and PENDRY, J. B., 1975, *Phys. Rev.*, **11,** 2795.
MATTHEISS, L. F., 1964, *Phys. Rev.* A, **134,** 970.
MUÑOZ-PAEZ, A., and SÁNCHEZ, E. M., 1992, Daresbury Laboratory Annual Report 1991–1992, p. 98.
MUSTRE DE LEON, J., YACOBY, Y., STERN, E. A., REHR, J. J., and DELL'ARRICCIA, M., 1989, *Physica* B, **158,** 263.
NATOLI, C. R., and BENFATTO, M., 1986, *J. Phys., Paris*, **47,** C8–11.
NORMAN, J. G., 1974, *Molec. Phys.*, **81,** 1191.
READ, M., and SANDSTRÖM, M., 1992, Daresbury Laboratory Annual Report 1990/1991, p. 194.
RUIZ-LÓPEZ, M. F., BOHR, F., FILIPPONI, A., DI CICCO, A., TYSON, T. A., BENFATTO, M., and NATOLI, C. R., 1991, *Proceedings of the Sixth International Conference on X-ray Absorption Fine Structure*, edited by S. S. Hasnain (Chichester, West Sussex: Ellis Horwood), p. 75.
RUIZ-LÓPEZ, M. F., LOOPS, M., GOULON, J., BENFATTO, M., and NATOLI, C. R., 1988, *Chem. Phys.*, **121,** 419.
SANCHEZ DEL RIO, M., GARCIA, J., BURATTINI, E., BENFATTO, M., and NATOLI, C. R., 1990, *Proceedings of the Second European Conference on Progress in X-ray Synchrotron Radiation Research*, edited by A. Balerna, E. Bernieri and S. Mobilio (Bologna: Societa' Italiana di Fisica), p. 35.
SANDSTROM, D. R., DODGEN, H. W., and LYTLE, F. W., 1977, *J. chem. Phys.*, **67,** 473.
SANDSTROM, D. R., and LYTLE, F. W., 1979, *A. Rev. phys. Chem.*, **30,** 215.
TEO, B. K., 1986, *EXAFS: Basic Principles and Data Analysis* (Berlin: Springer), 350 p.
TYSON, T. A., 1991, Ph.D. Thesis, Stanford University.
VEDRINSKII, R. V., BUGAEV, L. A., and LEVIN, I. G., 1988, *Phys. Stat. sol.* (b), **150,** 307.